Journal of Molecular Spectroscopy **210,** 250–258 (2001)
doi:10.1006/jmsp.2001.8453, available online at http://www.idealibrary.com on IDEAL®

Submillimeter-Wave Spectroscopy of TiCl in the Ground Electronic State

A. Maeda,* T. Hirao,† P. F. Bernath,† and T. Amano*

*Institute for Astrophysics and Planetary Sciences, Ibaraki University, 2-1-1 Bunkyo, Mito 310-8512, Japan; and †Department of Chemistry, University of Waterloo, Waterloo, Ontario, Canada N2L 3G1

Received July 9, 2001; in revised form September 13, 2001

The submillimeter-wave rotational transitions of TiCl in the ground state were observed using a double-modulation technique. TiCl was generated in a DC-discharge of a mixture of $TiCl_4$ vapor (less than 1 mTorr) and Ar buffer gas (80 mTorr) at a current of 200 mA. The $^4\Phi_{3/2}$, $^4\Phi_{5/2}$, $^4\Phi_{7/2}$, and $^4\Phi_{9/2}$ spin components of $Ti^{35}Cl$ ($v = 0, 1, 2$) and $Ti^{37}Cl$ ($v = 0$) were detected. The data were analyzed using effective rotational constants for each spin component as well as with the usual $\mathbf{N}^2$ reduced Hamiltonian. Recent Fourier transform and laser data were included in our fits and we confirm that the ground state of TiCl is a $^4\Phi_r$ electronic state.

I. INTRODUCTION

Although gas phase spectroscopy has been applied to transition-metal-containing molecules for a long time, structural information is still limited. Most metals have very high melting points that prevent the production of sufficient gaseous samples. Another important factor is the complexity of their electronic spectra. Because transition metal atoms have an open *d* shell, there is often a high density of close-lying electronic states with high spin multiplicitlies and large orbital angular momenta. As a result, spectra are dense, and sometimes the close states severely perturb each other. The molecules tend to be heavy and have small rotational constants, making the rotational lines difficult to resolve. These factors often lead to incorrect or ambiguous assignments.

TiCl is a typical transition-metal-containing molecule. Since the first spectroscopic detection by Fowler in 1907 in the region 400–420 nm (*1*), the observed complex band structure has caused controversy (*2–10*). More and Parker (*2*) attributed strong bands in the region 400–420 nm to a doublet system in their vibrational analysis. Rao (*3*) revised the electronic assignments to a $^4\Pi$-$^4\Sigma^-$ transition. Following Rao (*3*), Shenyavskaya *et al.* (*4*) investigated the possibility of different assignments, but they retained the electronic assignment as a $^4\Pi$-$^4\Sigma^-$. Chatalic *et al.* (*5*), and Diebner and Kay (*6*) each proposed similar assignments. Later, Lanini (*7*) carried out a rotational analysis for a few strong bands and suggested they were $^2\Pi$–$^2\Delta$ transitions. Phillips and Davis (*8*) classified a number of bands in the region 409.5–420 nm into four $\Delta\Omega = 1$ doublet–doublet transitions, but they did not specify the quantum number Λ for the upper and lower states.

It is only recently that Ram *et al.* (*11*) observed the electronic spectra of the isovalent TiF by Fourier transform spectroscopy and laser excitation spectroscopy. They obtained the energy separation between $X^4\Phi_{5/2}$ and $X^4\Phi_{3/2}$ spin components and identified the lower state of the emission spectra as the ground $X^4\Phi$ state. This assignment agreed with the results of recent *ab initio* calculations on TiF (*12, 13*). Following the spectroscopic study of TiF (*11*), Ram and Bernath recorded Fourier transform (FT) emission spectra of TiCl (*9*). They proposed assignments for bands in the region 3 000–12 000 cm^{-1} as $G^4\Phi$–$X^4\Phi$, $G^4\Phi$–$C^4\Delta$, and $C^4\Delta$–$X^4\Phi$, by analogy with TiF and TiH. They also predicted that the 420-nm bands were due to a $^4\Gamma$–$X^4\Phi$ transition, from their assignment of the infrared bands. Most recently, this prediction was supported by Imajo *et al.* (*10*), who recorded the emission spectra in the 420-nm region using a Fourier transform spectrometer.

Several theoretical calculations for TiCl have been reported (*12, 14–16*). Boldyrev and Simons calculated low-lying electronic states of TiCl as well as TiF using coupled cluster methods such as QCISD, QCISD(T), CCSD, and CCSD(T) (*12*). According to these calculations, the ground state is $^4\Phi$, but the $^4\Sigma^-$ and $^2\Delta_r$ states were predicted to be only a few thousand wavenumbers above the ground state. They also computed the bond length ($r_e = 2.311$ Å at a CCSD(T)/6-311 + +G(2*d*, 2*f*) level), the harmonic vibrational wavenumbers ($\omega_e = 393$ cm^{-1}), and the dipole moment ($\mu_e = 3.863$ D at a QCISD/6-311 + +G(*d*, *f*) level). Focsa *et al.* (*14*) compared the results calculated with ligand field theory (LFT) and density functional theory (DFT) for TiCl and $TiCl^+$. They suggested that the ground state was $^4\Phi$ on the basis of both LFT and DFT calculations. LFT provided the excitation energies for the $^4\Delta$–$X^4\Phi$ and $^4\Phi$–$X^4\Phi$ transitions of 3 100 and 11 600 cm^{-1}, respectively, which were comparable to observed values, 3 300 and 10 900 cm^{-1} (*9*). They also pointed out that the ground state was a mixture of 69% of $3d^2(^3F)4s$ from $Ti^+(^4F)$ and 31% of $3d^3$ from $Ti^+(^4F)$ in the LFT calculation. Sakai *et al.* (*15*) investigated the low-lying electronic states of TiCl and ZrCl by CASSCF, MRSDCI, and MRCPA

0022-2852/01 $35.00

methods. Although they predicted that the ground state of TiCl was $^4\Phi$, they said that the ground state is relatively pure (91.9% of a single configuration), unlike the LFT results of Focsa *et al.* (*14*) Very recently, Ram *et al.* (*16*) reinvestigated ZrCl and calculated the electronic structure of the isovalent TiCl, ZrCl, and HfCl molecules at the CASSCF/CMRCI level. They revised the previous spectroscopic results for ZrCl (*17, 18*) and concluded that ZrCl and HfCl have $^2\Delta$ ground states, as suggested by Sakai *et al.* for ZrCl (*15*), in contrast to the $^4\Phi$ state of TiCl. They calculated that the ground state of TiCl was a mixture of $3d^2(^3\mathrm{F})4s$ (86%) of Ti^+ and $3d^3$ (14%) of Ti^+.

All of these *ab initio* calculations support the previous FT emission results (*9, 10*) and suggest that the TiCl molecule has a relatively pure $^4\Phi$ ground state. There is, however, still no experimental proof of the identity of the ground state, because the experimental conclusions were derived only from emission spectra (*9, 10*) and by analogy with TiF and TiH.

In this study, we have observed pure rotational absorption transitions ranging from $J'' = 41.5$ to 62.5 in the region 400–600 GHz for two chlorine isotopic species, $Ti^{35}Cl$ and $Ti^{37}Cl$, for four different spin components. Also, lines in the $v = 1$ and 2 excited vibrational states for $Ti^{35}Cl$ were detected. In this paper, we present the $^4\Phi$ effective rotational constants and the molecular structure, and confirm the assignment of the ground state of TiCl.

II. EXPERIMENTAL

Figure 1 is a schematic diagram of the experimental setup. The absorption spectra of TiCl were detected using a submillimeter-wave spectrometer with a double modulation technique (*19*) at Ibaraki University. The radiation was generated by two backward-wave oscillator (BWO) tubes that covered 400–600 GHz with some gaps. The double modulation method enables a very effective baseline subtraction (*19*). Consequently, weak TiCl lines were made more recognizable and the line positions were determined more precisely than is possible with ordinary source modulation. The source modulation and discharge modulation frequencies were set at 40 kHz and 28.3 Hz, respectively.

The discharge cell was a 1.5-m-long and 40-mm-inner diameter Pyrex tube with a cube corner reflector at the end of the cell. The polarization of the submillimeter-wave radiation was rotated 90° by the mirror. The radiation back to the entrance of the cell was reflected by a beam splitter and detected with a helium-cooled InSb detector.

The TiCl molecules were produced in a DC-glow discharge through a flowing mixture of $TiCl_4$ vapor and Ar. A commercial $TiCl_4$ (Aldrich, 99%) sample was placed in a glass tube at room temperature. The pressure of $TiCl_4$ was controlled with a Teflon valve and monitored with a Baratron pressure gauge at the exit of the cell. The cell was evacuated with a mechanical booster pump backed by an oil-free rotary pump.

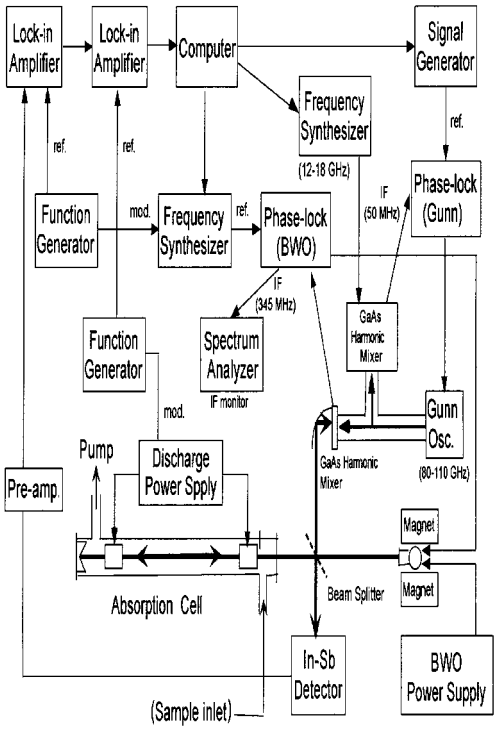

FIG. 1. A schematic diagram of the double-modulation submillimeter-wave spectrometer system.

At the beginning, the search for the pure rotational spectra was guided by the effective molecular constants obtained from the FT emission work (*9, 10*). If the ground state is really $^4\Phi_r$, then the lines of the $\Omega = 3/2$ component should be stronger than those of the other spin components. Considering the output power of the BWO and the intensity distribution for the different spin components, we started to search for the $\Omega = 3/2$ spin component of the $J = 45.5 \leftarrow 44.5$ transition around 439.40 GHz. The initial vapor pressure of $TiCl_4$ was approximately 1 mTorr or more. At least 60 mTorr of Ar buffer gas was necessary to sustain a stable DC discharge with a current of 100 mA. The absorption cell was cooled to 0°C. After some manipulation of the chemistry and a search in a wider frequency range, we found one weak absorption line at 439.37 GHz, which was about 30 MHz lower than the prediction. After the first detection and the optimization of the discharge conditions, we investigated other frequency regions, taking into account a systematic shift (30 MHz) found for our initial prediction, and we found absorption lines with similar intensities. We also tried to find the other spin components using the predicted frequencies, and we obtained spectra for all spin components. Because the absorption lines could not be produced without $TiCl_4$ vapor, and the line positions were found with a systematic deviation of about 30 MHz from the initial prediction, we concluded that these absorption lines were due to the rotational transitions of TiCl, and the ground electronic state of TiCl must be a quartet.

Ultimately, the optimum conditions for producing TiCl were found. The optimum pressure of $TiCl_4$ was less than 1 mTorr with

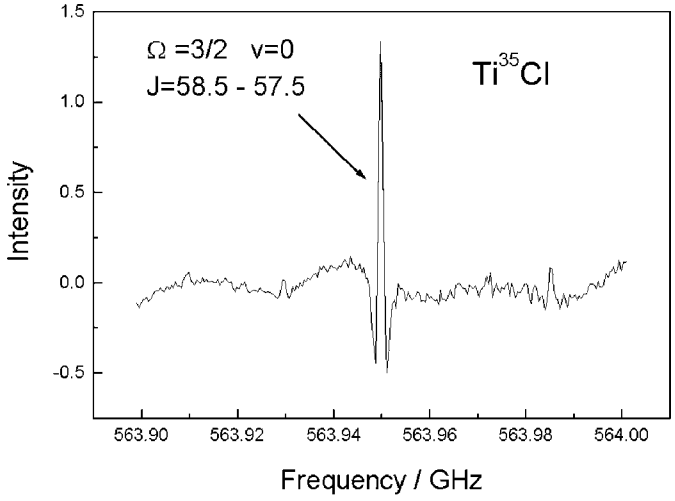

FIG. 2. An example of the rotational spectra of TiCl recorded with a double-modulation submillimeter-wave spectrometer. Several weak features remain unidentified.

~80 mTorr Ar buffer. The DC discharge current was optimized at 200 mA. The cell was at room temperature although generally speaking, radical species can be more easily detected at a lower temperature. Note that the pressure of $TiCl_4$ critically affected the production of TiCl. The optimum pressure was eventually established by observing the discharge color. When the color was radiant blue, the spectra appeared strongly. Figure 2 shows an example of the recorded double-modulated spectra.

Following the detection of the $v = 0$ state of $Ti^{35}Cl$, the measurements were extended to the $v = 0$ level of $Ti^{37}Cl$ and the $v = 1$ level of $Ti^{35}Cl$ by using the molecular constants from the FT measurements (*9, 10*). It turned out that the signals were strong enough to observe rotational transitions in the $v = 2$ level of $Ti^{35}Cl$ and the assignments were rather straightforward. The relative intensity of the spectra of $Ti^{37}Cl$ and in the first excited vibrational state of $Ti^{35}Cl$ appeared to be about 2/3 of the corresponding lines of the ground vibrational state of $Ti^{35}Cl$. Also, the intensity of lines with different Ω values varied gradually, as theoretically expected for Hund's case (a) molecules.

During the survey, several lines, which have a slightly different optimum reaction condition from that of TiCl, were also discovered. They are probably due to other Ti-containing molecules and will be investigated in the future. Tables 1–4 list the observed transition frequencies of $Ti^{35}Cl$ ($v = 0, 1, 2$) and $Ti^{37}Cl$ ($v = 0$). Three sets of measured frequencies of the upward and downward scans were averaged to obtain precise transition frequencies. The line accuracy is expected to be about ±50 kHz.

III. ANALYSIS

The analysis was carried out in three steps. First, effective polynomial energy formulas were applied separately for the four spin components. This procedure provided an estimate of the spin-orbit coupling constant A_{so}. Secondly, the 4×4 energy matrix was set up for a $^4\Phi$ state with the $\mathbf{N}^2$ reduced Hamiltonian using Hund's case (a) basis functions and used to fit the data. Finally, we combined all spectroscopic data available to derive more reliable molecular constants in the ground state.

III.1. Effective Polynomial Formula

The effective rotational constants for the four different spin components were determined by fitting the lines of each spin component separately to the simple energy expression

$$F = T + B_{eff}\,J(J+1) - D_{eff}[J(J+1)]^2, \qquad [1]$$

where B_{eff} and D_{eff} are effective rotational and centrifugal

TABLE 1
Transition Frequencies of $Ti^{35}Cl$ in the Ground Vibrational State (in GHz)[a]

Species	Transition	Ω = 3/2	5/2	7/2	9/2
	42.5 ← 41.5	410.536113 (47)	411.664920 (38)	412.797547 (02)	413.945779 (02)
	43.5 ← 42.5	—	—	422.463397 (37)	423.637735 (20)
	44.5 ← 43.5	429.762051 (11)	430.942015 (66)	432.125993 (49)	433.326333 (27)
	45.5 ← 44.5	439.370154 (61)	440.575700 (43)	441.785311 (15)	443.011541 (67)
	46.5 ← 45.5	448.975018 (52)	450.205993 (52)	451.44125 (13)	452.693202 (56)
	47.5 ← 46.5	458.576500 (58)	—	—	—
	48.5 ← 47.5	468.174597 (03)	469.456258 (08)	470.742219 (32)	472.045728 (42)
$Ti^{35}Cl$	49.5 ← 48.5	477.769130 (01)	479.076037 (00)	480.387322 (48)	481.716482 (79)
($v = 0$)	50.5 ← 49.5	487.360048 (25)	488.692152 (04)	490.028666 (38)	491.38342 (11)
	51.5 ← 50.5	—	498.304605 (77)	499.66607 (11)	—
	56.5 ← 55.5	544.826311 (06)	546.307834 (19)	—	—
	57.5 ← 56.5	554.390091 (19)	555.896274 (09)	557.407375 (16)	558.938719 (11)
	58.5 ← 57.5	563.949727 (07)	565.480473 (07)	567.016117 (48)	568.572404 (45)
	59.5 ← 58.5	573.505168 (52)	575.060360 (40)	576.620520 (43)	578.201624 (45)
	60.5 ← 59.5	583.056228 (46)	584.635839 (61)	586.220462 (17)	587.826229 (95)
	61.5 ← 60.5	592.602924 (63)	594.206842 (79)	595.815803 (34)	597.446233 (97)
	62.5 ← 61.5	602.145114 (35)	—	—	—

[a] Values in parentheses represent $\nu_{obs.}$-$\nu_{calc.}$ in the last significant digits.

TABLE 2
Transition Frequencies of $Ti^{35}Cl$ in the First Vibrational State (in GHz)[a]

Species	Transition	$\Omega = 3/2$	5/2	7/2	9/2
	42.5 ← 41.5	408.508953 (90)	409.625733 (46)	410.746570 (05)	411.882872 (80)
	43.5 ← 42.5	418.075775 (53)	419.217900 (43)	420.364152 (21)	421.526195 (01)
	44.5 ← 43.5	427.639427 (40)	428.806823 (62)	429.978497 (06)	431.166300 (85)
	48.5 ← 47.5	465.861010 (03)	467.128975 (07)	468.401579 (64)	469.691445 (43)
$Ti^{35}Cl$	49.5 ← 48.5	475.407755 (30)	476.700738 (10)	477.998395 (70)	479.313605 (49)
($v = 1$)					
	58.5 ← 57.5	561.158492 (29)	562.672886 (30)	564.192604 (34)	565.732550 (21)
	59.5 ← 58.5	570.666101 (55)	572.204696 (34)	573.748616 (25)	575.313242 (04)
	60.5 ← 59.5	580.169334 (23)	581.732094 (32)	583.300267 (23)	584.889300 (33)
	61.5 ← 60.5	589.668225 (35)	591.255009 (09)	592.847260 (45)	594.460717 (61)
	62.5 ← 61.5	599.162650 (46)	600.773333 (51)	602.389710 (05)	604.02739 (10)

[a] Values in parentheses represent $\nu_{obs.}$-$\nu_{calc.}$ in the last significant digits.

TABLE 3
Transition Frequencies of $Ti^{35}Cl$ in the Second Vibrational State (in GHz)[a]

Species	Transition	$\Omega = 3/2$	5/2	7/2	9/2
	44.5 ← 43.5	425.521790 (39)	—	427.835879 (69)	429.011109 (19)
	45.5 ← 44.5	435.034492 (32)	436.214170 (60)	437.398599 (10)	438.599358 (53)
	46.5 ← 45.5	444.543976 (19)	445.748523 (81)	446.958037 (61)	448.184013 (32)
	47.5 ← 46.5	454.050086 (04)	455.279536 (01)	456.513877 (41)	457.764994 (88)
	48.5 ← 47.5	—	—	—	467.34271 (18)
$Ti^{35}Cl$	54.5 ← 53.5	520.49200 (13)	—	523.300282 (36)	524.726196 (09)
($v = 2$)	55.5 ← 54.5	529.968626 (32)	531.394316 (83)	532.825345 (61)	534.275890 (44)
	56.5 ← 55.5	539.441023 (10)	540.890870 (07)	542.346297 (11)	543.821316 (81)
	57.5 ← 56.5	548.909347 (20)	550.383256 (55)	551.862955 (05)	—
	59.5 ← 58.5	567.833418 (15)	569.355448 (83)	570.883117 (32)	—
	60.5 ← 59.5	577.289035 (18)	—	—	—
	61.5 ← 60.5	586.74033 (12)	—	—	—

[a] Values in parentheses represent $\nu_{obs.}$-$\nu_{calc.}$ in the last significant digits.

TABLE 4
Transition Frequencies of $Ti^{37}Cl$ in the Ground Vibrational State (in GHz)[a]

Species	Transition	$\Omega = 3/2$	5/2	7/2	9/2
	43.5 ← 42.5	407.126263 (97)	408.210831 (15)	—	410.401115 (44)
	44.5 ← 43.5	416.441094 (81)	417.549696 (32)	418.661663 (68)	419.788675 (63)
	45.5 ← 44.5	425.752905 (57)	426.885454 (68)	428.021660 (58)	429.17299 (13)
	46.5 ← 45.5	435.061565 (86)	436.218079 (81)	437.378238 (19)	438.55393 (10)
	47.5 ← 46.5	444.367156 (18)	445.547560 (11)	446.731613 (11)	447.931480 (40)
$Ti^{37}Cl$	51.5 ← 50.5	—	482.831557 (07)	484.110850 (44)	485.407055 (94)
($v = 0$)	52.5 ← 51.5	490.844972 (63)	492.143806 (04)	493.44678 (11)	—
	53.5 ← 52.5	500.130003 (01)	501.452394 (03)	502.778870 (33)	—
	59.5 ← 58.5	555.761739 (97)	557.223656 (87)	—	560.175378 (45)
	60.5 ← 59.5	565.019807 (16)	566.504692 (25)	567.994123 (10)	569.50275 (10)
	61.5 ← 60.5	574.273819 (02)	575.781744 (79)	577.293979 (63)	578.825964 (56)
	62.5 ← 61.5	583.523743 (91)	585.054330 (15)	586.589568 (56)	588.144662 (96)
	63.5 ← 62.5	592.769220 (08)	594.322725 (38)	595.880772 (17)	597.458908 (89)

[a] Values in parentheses represent $\nu_{obs.}$-$\nu_{calc.}$ in the last significant digits.

TABLE 5
Effective Molecular Constants for TiCl in the Ground State[a]

	Constants	$\Omega = 3/2$	5/2	7/2	9/2
$Ti^{35}Cl$ ($v = 0$)	B_{eff}/MHz	4 840.74025 (44)	4 854.23883 (48)	4 867.78647 (45)	4 881.52677 (45)
	D_{eff}/kHz	3.018068(71)	3.078710(80)	3.140419(76)	3.204522(76)
previous value[b]	B_{eff}/MHz	4 841.05 (16)	4 853.78 (24)	4 867.34 (20)	4 881.48 (14)
	D_{eff}/kHz	3.082 (23)	2.932 (45)	3.085 (39)	3.207 (20)
$Ti^{35}Cl$ ($v = 1$)	B_{eff}/MHz	4 816.90091 (57)	4 830.25597 (57)	4 843.66200 (57)	4 857.25838 (57)
	D_{eff}/kHz	3.020686(90)	3.080784(90)	3.141688(27)	3.205051(27)
previous value[b]	B_{eff}/MHz	4 816.99 (18)	4 829.63 (24)	4 843.10 (21)	4 857.24 (15)
	D_{eff}/kHz	3.046 (27)	2.875 (51)	3.061 (45)	3.204 (23)
$Ti^{35}Cl$ ($v = 2$)	B_{eff}/MHz	4 793.11854 (76)	4 806.3263 (12)	4 819.59371 (89)	4 833.0479 (11)
	D_{eff}/kHz	3.02364 (12)	3.08269 (17)	3.14340 (15)	3.20616 (20)
$Ti^{37}Cl$ ($v = 0$)	B_{eff}/MHz	4 690.34609 (60)	4 703.01795 (58)	4 715.73196 (57)	4 728.62149 (60)
	D_{eff}/kHz	2.836000(93)	2.890600(92)	2.945937(97)	3.003412(93)
previous value[c]	B_{eff}/MHz	4 690.70 (87)			
	D_{eff}/kHz	3.15 (33)			

[a] Values in parentheses indicate one standard deviation in the last significant digits.
[b] From Ref. (*9*).
[c] From Ref. (*10*).

distortion constants, respectively. The effective molecular constants thus obtained are listed in Table 5. The effective rotational constants of the four spin components show good agreement and great improvement over the previous values from electronic FT emission spectra (*9*, *10*).

The effective rotational constants for four spin components are given in terms of the rotational and spin–orbit constants as (*11*)

$$B_{eff}(3/2) = B\left(1 - \frac{B}{A}\right), \quad [2]$$

$$B_{eff}(5/2) = B\left(1 - \frac{B}{3A}\right), \quad [3]$$

$$B_{eff}(7/2) = B\left(1 + \frac{B}{3A}\right), \quad [4]$$

$$B_{eff}(9/2) = B\left(1 + \frac{B}{A}\right). \quad [5]$$

The spin–orbit and rotational constants obtained using Eqs. [2] to [5] for $Ti^{35}Cl$ in the $v = 0$ state were 1 159 GHz and 4 861.022 72(20) MHz, respectively. The spin–orbit constant is comparable to the value 1 104.99 GHz derived from a recent laser spectroscopic measurement (*20*). The spin–orbit parameter can also be estimated from the atomic metal ion parameter, ζ (*21*). According to recent theoretical calculations (*12*, *14–16*), the molecular electronic configuration of the ground state of TiCl can be well represented as $1\sigma^2 2\sigma^2 1\pi^4 3\sigma^1 1\delta^1 2\pi^1$, where the valence 3σ, 1δ, and 2π electrons are primarily from the $3d$ atomic orbital of Ti^+. If the TiCl orbitals containing the unpaired electrons are approximated as Ti^+ orbitals, then one obtains the relationship $A_{so}(X^4\Phi) \approx \zeta(Ti^+)/3$. If the atomic electronic configuration of Ti^+ is purely $3d^2 4s[^4F]$ and $\zeta(Ti^+) = 117$ cm^{-1} (*22*), then the molecular A_{so} is estimated to be 39 cm^{-1} (1 300 GHz), in excellent agreement with our value.

III.2. N^2 Reduced Hamiltonian

We fitted the data using the $\mathbf{N}^2$ reduced Hamiltonian (*23–25*) and the 4×4 matrix derived using Hund's case (a) basis functions. The Hamiltonian used is

$$\boldsymbol{H} = \boldsymbol{H}_{rot} + \boldsymbol{H}_{so} + \boldsymbol{H}_{rs} + \boldsymbol{H}_{ss} + \boldsymbol{H}_{so}^{(3)}, \quad [6]$$

where

$$\boldsymbol{H}_{rot} = B\boldsymbol{N}^2 - D\boldsymbol{N}^4 + H\boldsymbol{N}^6, \quad [7]$$

$$\boldsymbol{H}_{so} = \frac{1}{2}[A + A_D\boldsymbol{N}^2 + A_H\boldsymbol{N}^4, L_zS_z]_+, \quad [8]$$

$$\boldsymbol{H}_{rs} = (\gamma + \gamma_D\boldsymbol{N}^2 + \gamma_H\boldsymbol{N}^4)(\boldsymbol{N}\cdot\boldsymbol{S}), \quad [9]$$

$$\boldsymbol{H}_{ss} = \frac{1}{3}\left[\lambda + \lambda_D\boldsymbol{N}^2 + \lambda_H\boldsymbol{N}^4, 3S_z^2 - \boldsymbol{S}^2\right]_+, \quad [10]$$

$$\boldsymbol{H}_{so}^{(3)} = \frac{1}{2}\left[\eta + \eta_D\boldsymbol{N}^2 + \eta_H\boldsymbol{N}^4, L_zS_z\left(S_z^2 - \frac{3\boldsymbol{S}^2 - 1}{5}\right)\right]_+, \quad [11]$$

and

$$\boldsymbol{N} = \boldsymbol{J} - \boldsymbol{S}, \quad [12]$$

where $[x, y]_+$ stands for the anticommutator $xy + yx$.

TABLE 6
A Comparison of the Molecular Constants of $Ti^{35}Cl$ in the Ground Electronic State ($v = 0$ and 1)[a]

Constants	Set I	Set II	Set III
A_0/cm^{-1}	38.7[b,c]	37.213 22 (37)	37.195 45 (36)
A_{D0}/MHzx	−0.049 238 (72)	−0.221 8 (82)	−0.231 325 (49)
A_{H0}/Hz	−0.835 (12)	—	—
B_0/MHz	4 861.096 27 (24) [4 861.022 72][b]	4 860.92 (11)	4 861.096 28 (29)
D_0/kHz	3.110 414 (40)	3.082 (17)	3.110 405 (48)
λ_0/MHz	3 159.6 (24)	5 339. (10)	4 644. (11)
λ_{D0}/kHz	—	—	20.17 (14)
η_0/MHz	−331.8 (12)	—	−301.8 (13)
E_1/cm^{-1}	—	404.332 04 (86)	404.328 72 (34)
A_1/cm^{-1}	38.7[b,c]	37.204 65 (41)	37.187 91 (37)
A_{D1}/MHz	−0.048 664 (69)	−0.207 4 (86)	−0.232 879 (52)
A_{H1}/Hz	−0.843 (11)	—	—
B_1/MHz	4 837.042 61 (23) [4 836.969 04][b]	4 836.76 (11)	4 837.042 74 (31)
D_1/kHz	3.112 051 (36)	3.062 (19)	3.112 065 (49)
λ_1/MHz	3 111.6 (25)	5 393. (11)	4 689. (12)
λ_{D1}/kHz	—	—	21.16 (16)
η_1/MHz	−320.1 (13)	—	−292.3 (15)
$\bar{\sigma}_f$[d]	0.68	0.96	1.01

[a] All numbers in parentheses indicate standard deviations for the last significant digits.
[b] Estimated values from effective constants in Table 5. For more details, see text.
[c] Fixed values in the Set I fit.
[d] The dimensionless standard error,

$$\bar{\sigma}_f = \left\{ \frac{1}{N-M} \sum_{i=1}^{N} \left[\frac{\nu_{calc.}(i) - \nu_{obs.}(i)}{u(i)} \right]^2 \right\}^{1/2},$$

where $u(i)$ indicates an estimated uncertainty of the measurement, N is the number of data, and M the number of parameters used.

No cross transitions with $\Delta\Omega \neq 0$ were observed in our submillimeter-wave measurements, and thus the spin–orbit constant was fixed to our estimated values. The molecular constants thus determined for $Ti^{35}Cl$ ($v = 0, 1$) are listed as "Set I" in Table 6. The rotational constants compared well with the estimated values from formulas [2]–[5]. Note that we could also attain a similar quality of the fit without the third order spin–orbit coupling term (*25*), η[11], if a higher order centrifugal distortion term λ_H were included as an adjustable parameter.

III.3. Reanalysis of the Previous FT Measurement

Based on our confirmation of the ground state as $^4\Phi$, the C and G states (*9*) and a state lying around 23 000 cm^{-1} (*10*) should be $^4\Delta$, $^4\Phi$, and $^4\Gamma$, respectively. However, the $C^4\Delta$ and $G^4\Phi$ states of TiCl were analyzed only by using the effective energy formula [1], and the spacing between spin components was not known. A very recent laser experiment on [23.0]$^4\Gamma$–$X^4\Phi$ 0–0 transition (*20*) enables us to determine the intervals between $^4\Phi_{3/2}$, $^4\Phi_{5/2}$ and $^4\Phi_{7/2}$ in the ground state. We therefore decided to reanalyze the $C^4\Delta$–$X^4\Phi$ 0–0, $G^4\Phi$–$X^4\Phi$ 0–0 and 0–1, and $G^4\Phi$–$C^4\Delta$ 0–0 transitions (*9*) with our submillimeter-wave spectra and the ground state combination differences of the [23.0]$^4\Gamma$–$X^4\Phi$ 0–0 transition from the unpublished laser experiments (*20*). The $G^4\Phi$–$X^4\Phi$ 1–0 transition was available but excluded from our fit because the band is strongly perturbed.

In the first fit, only the Fourier transform data and the combination differences from the laser experiment were included. In the fit, the line accuracy was set to 150 MHz for FT emission (*9*) and 200 MHz for laser combination differences (*20*). An effective Hamiltonian [6]–[12] (*23–25*) was also utilized for the $C^4\Delta$ state. The molecular constants for the ground electronic state ($v = 0, 1$) obtained from this fit are listed as "Set II" in Table 6. The spin–orbit coupling constant in the $X^4\Phi(v = 0)$ state was determined to be 37.213 22(37) cm^{-1} (1 115.6243(111) GHz), in a good agreement with the predicted value, 1 159 GHz. In this fit, the predicted line positions agree with those measured within the estimated experimental uncertainties, while η_v is too small to be determined from the FT and laser data alone.

In the second fit, we included in addition our submillimeter-wave data in the data set. The obtained molecular constants in the ground state ($v = 0, 1$) are listed as "Set III" in Table 6, and those for the electronically excited states are in Table 8. When we included the submillimeter-wave data in our fit, η_v appeared to be necessary in the fit, indicating that η_v is determined mainly from the high precision submillimeter-wave data. The η_v constant is needed to account for deviations from a pure Hund's case

TABLE 7
Molecular Constants for $Ti^{35}Cl$ ($v = 2$) and $Ti^{37}Cl$ ($v = 0$) in the Ground State[a]

Constants	$Ti^{35}Cl$ ($v = 2$)	$Ti^{37}Cl$($v = 0$)
A/cm^{-1}	37.180 37[b]	37.195 45[b]
	[38.7][c]	[38.7][c]
A_D/MHz	−0.234 618 (32)	−0. 216 683 (28)
B/MHz	4 813. 044 44 (54)	4 709. 451 31 (37)
	[4 812.970 34][c]	[4 709.384 02][c]
D/kHz	3. 113 853 (93)	2. 918 992 (59)
λ/MHz	4 733 [b]	4 644 [b]
λ_D/kHz	22.443 (56)	19.596 (45)
η/MHz	−282. 4 (23)	−295. 0 (17)

[a] Values in parentheses indicate one standard deviation for the last significant digits.
[b] Fixed. For more details, see text.
[c] Estimated values from our effective constants in Table 5.

(a) state and, consequently, A_v and λ_v differ significantly from the values in Set II of Table 6. These differences in molecular constants were caused by the inclusion of pure rotational transitions and also because η_v is considered in Set III but not Set II. None of the transitions observed provide distinct information on the spin–spin interaction. The relative locations of the different spin components are not quite fixed from the observations. In this respect, these spin coupling constants should be regarded as effective parameters. Although the molecular constants thus obtained are still somewhat effective, these constants in Set III should be more realistic than those in Sets I and II. Note that the rotational constant, B_v, in Sets I and III are almost equal, indicating that changing A_v and λ_v does not influence B_v, despite the formulas [13]–[16] given in the next section.

TABLE 8
Molecular Constants for $Ti^{35}Cl$ in $C^4\Delta$ and $G^4\Phi$ States in Units of cm^{-1}[a]

Constants	$C^4\Delta$ ($v = 0$)	$G^4\Phi$ ($v = 0$)
$E\times 10^3$	3.302 830 41 (46)	10.909 294 26 (45)
A	34.509 06 (56)	32.285 44 (38)
	[29][a]	[26][a]
$A_D\times 10^5$	6.587 (16)	3.658 6 (105)
$A_H\times 10^9$	−0.816 (30)	−1.915 (20)
B	0.157 970 42 (93)	0.150 827 46 (78)
	[0.157 97][a]	[0.150 82][a]
$D\times 10^7$	0.825 9 (40)	1.253 7 (35)
$H\times 10^{12}$	−0.570 (48)	1.310 (46)
λ	−1.315 83 (41)	−1.136 18 (40)
$\lambda_D\times 10^5$	−8.197 (39)	5.474 (24)
$\lambda_H\times 10^8$	−1.387 6 (122)	−0.349 8 (57)
η	−0.446 39 (22)	0.031 094 (145)
$\eta_D\times 10^5$	–	−1.628 1 (76)

Note. All numbers in parentheses indicate standard deviations for the last significant digits.
[a] Estimated values from Ref. (*9*).

For $Ti^{35}Cl$ ($v = 2$) and $Ti^{37}Cl$ ($v = 0$), there is no information available about the intervals between the four spin components. Because of this, A_v and λ_v for $Ti^{37}Cl$ ($v = 0$) were constrained to the values obtained for $Ti^{35}Cl$ ($v = 0$) from Set III in Table 6. In the case of $Ti^{35}Cl$ ($v = 2$), A_v and λ_v were fixed to the values estimated from a usual linear relationship, $A_v = A_e - \alpha_A(v + \frac{1}{2})$, with A_v and λ_v for $Ti^{35}Cl$ ($v = 0, 1$) from Set III in Table 6. The results are listed in Table 7.

IV. DISCUSSION

The rotationless energy level structure for the spin components in a $^4\Phi$ state, excluding the spin–rotation interaction and off-diagonal terms, can be represented as follows:

$$F(\Omega = 3/2) = T - \frac{9}{2}A + 2\lambda - \frac{9}{10}\eta + \frac{33}{4}B, \quad [13]$$

$$F(\Omega = 5/2) = T - \frac{3}{2}A - 2\lambda + \frac{27}{10}\eta + \frac{25}{4}B, \quad [14]$$

$$F(\Omega = 7/2) = T + \frac{3}{2}A - 2\lambda - \frac{27}{10}\eta + \frac{1}{4}B, \quad [15]$$

$$F(\Omega = 9/2) = T + \frac{9}{2}A + 2\lambda + \frac{9}{10}\eta - \frac{39}{4}B. \quad [16]$$

These equations suggest that A_v, λ_v, and η_v are difficult to be determined independently, unless cross transitions with $\Delta\Omega \neq 0$ are observed and the three spin–orbit intervals are derived. As shown in the analysis, λ_v and η_v were determined only from the submillimeter-wave data (Set I in Table 6). Because λ_v and η_v constants are of the same order of magnitude as the rotational constant, B_v, the deviation from the case (a) in higher J-rotational states, although small, is not negligible. For example, if λ_v is varied from 3 GHz (0.10 cm^{-1}) to 4.5 GHz (0.15 cm^{-1}) with all other parameters unchanged, the effective term values, [13]–[16], should vary by $2 \times |\Delta\lambda_v| = 3$ GHz (0.10 cm^{-1}) for any J, when the deviation from the case (a) is completely neglected. However, when the effect of the off-diagonal rotational part of the Hamiltonian is included, the effect of λ_v on the term value at a high J such as $J = 60.5$ is reduced by about 133 MHz. Because of this J dependence due to the departure from pure case (a), "effective" λ_v and η_v can be determined, even if cross transitions with $\Delta\Omega \neq 0$ are not available.

The rotational constants for the $v = 0$, 1, and 2 from Tables 6 and 7 resulted in the equilibrium constants $B_e =$ 4 873.143 77(72) MHz, $\alpha_e = 24.108\,78(122)$ MHz, and $\gamma_e = 27.62(44)$ kHz. The r_e structure of TiCl is $r_e =$ 2.264 623 45 (15) Å (Table 9), which is significantly smaller than the values determined by *ab initio* calculations, 2.311 Å, 2.370 Å, and 2.319 Å at CCSD(T) (*12*) end CASSCF and MRSDCI + Q (*15*) levels, respectively. The r_0 structure in the C and G excited states was obtained as 2.297 237 9(68) Å and 2.296 823 3(57) Å, respectively. The obtained r_0 structure in

TABLE 9
The Equilibrium Structure of $Ti^{35}Cl$

Constants	Present work	FT emission[a]	CCSD(T)[b]	MRSDCI+Q[c]
r_e/Å	2.264 623 45 (15)	2.264 7	2.311	2.319
B_e/MHz	4 873.143 77 (72)	—	—	4 646
α_e/MHz	24.108 78 (122)	24.0	—	21.6
γ_e/kHz	27.62 (44)	—	—	—

[a] Taken from Ref. (*9*).
[b] Taken from Ref. (*12*).
[c] Taken from Ref. (*15*).

the C state is again shorter than the 2.38 Å obtained in the DFT calculation (*14*).

According to the recent calculations (*14–16*), the $X^4\Phi_r$ and $G^4\Phi_r$ states are both mixtures of two Ti^+ configurations, $3d^24s$ from $Ti^+(^4F)$ and $3d^3$ from $Ti^+(^4F)$. The recent LFT calculation (*14*) also suggested that the $3d^24s$ configuration from $Ti^+(^4F)$ dominates in the ground state, while the G state has the opposite mixing ratio. Taking mixing ratios from latest calculation (*16*), the basis functions of the ground and G states can be written

$$|X^4\Phi_r\rangle = b|3d^24s\rangle + \sqrt{1-b^2}|3d^3\rangle, \quad [17]$$

$$|G^4\Phi_r\rangle = \sqrt{1-b^2}|3d^24s\rangle + b|3d^3\rangle, \quad [18]$$

where $b^2 = 0.86$. On the other hand, the dominant configuration of the $C^4\Delta_r$ state is $3d^24s$ from $Ti^+(^4F)$ (*14*). If the ground state spin–spin interaction arises only from the second order perturbation of the spin–orbit interaction between the $X^4\Phi_r$ and $C^4\Delta_r$ states, one can obtain the effective spin–spin interaction parameter of the ground state by using perturbation theory (*23*):

$$\lambda^{(2)} = \frac{30(2S-2)!}{(2S+3)!}\sum_{\Sigma}\left[\{3\Sigma^2 - S(S+1)\} \times \sum_{n'\Lambda'\Sigma'} \frac{\left|\langle X^4\Phi_r, \Lambda=3, S=\frac{3}{2}, \Sigma|H^e_{so}|n', \Lambda', S', \Sigma'\rangle\right|^2}{(E_X - E_{n'})}\right]. \quad [19]$$

Taking the matrix elements from the literature (*14, 26*), $\lambda^{(2)}$ is calculated to be $+0.277$ cm^{-1}, which is significantly larger than our observed value in the ground state ($+0.155$ cm^{-1}, from Table 6, Set III). Recent *ab initio* calculations (*12, 15, 16*) predict that there is a low-lying $^2\Delta_r$ state approximately 3 000 cm^{-1} higher than the ground state. It was also predicted that the electronic configuration of the $^2\Delta_r$ state is almost pure $3d^24s$ from $Ti^+(^4F)$ (*14, 16*). Assuming the $^2\Delta_r$ state is responsible for the difference between the observed ($+0.155$ cm^{-1}) and calculated values from the $C^4\Delta_r$ state ($+0.227$ cm^{-1}), the term value of the $^2\Delta_r$ state is estimated from Eq. [19] to be 1 370 cm^{-1}, comparable with the latest *ab initio* calculations (*12, 15, 16*).

The η constant arises mainly from a third order spin–orbit perturbation (*24*):

$$\eta_n^{(3)} = \frac{2800(2S-3)!}{\Lambda(2S+4!)}\sum_{\Sigma}\left[\left\{\Sigma^3 - \frac{1}{5}\Sigma(3S^2+3S-1)\right\} \times \sum_{n'\Lambda'\Sigma'n''\Lambda''\Sigma''} \times \frac{\langle n\Lambda S\Sigma|H^e_{so}|n'\Lambda'S'\Sigma'\rangle\langle n'\Lambda'S'\Sigma'|H^e_{so}|n''\Lambda''S''\Sigma''\rangle\langle n''\Lambda''S''\Sigma''|H^e_{so}|n\Lambda S\Sigma\rangle}{(E_n - E_{n'})(E_n - E_{n''})}\right]. \quad [20]$$

Assuming only the $C^4\Delta_r$ and $^2\Delta_r$ states are dominant intermediate states for the ground state, the interaction can occur only through $X^4\Phi_{3/2} \sim C^4\Delta_{3/2} \sim^2 \Delta_{3/2} \sim X^4\Phi_{3/2}$ or $X^4\Phi_{5/2} \sim C^4\Delta_{5/2} \sim {}^4\Delta_{5/2} \sim X^4\Phi_{5/2}$ because of the selection rule of the matrix elements in formula [20]. In this case, $\eta^{(3)}$ is calculated to be -0.005 cm^{-1}, while the observed value is -0.010 cm^{-1}. Although there can be more states such as $^2\Phi$ and $G^4\Phi$ involved in the third order perturbation, the discrepancy is probably because the obtained η in the ground state is still effective.

V. CONCLUSION

The pure rotational transitions in the ground state for $J'' = 41.5$–62.5 were obtained for four spin components by using a submillimeter-wave spectrometer with double modulation. By fitting the data with a $^4\Phi$ Hamiltonian, more accurate molecular constants have been determined. Our measurements will be useful in searching for TiCl in interstellar space. We have confirmed that the ground state of TiCl is a $^4\Phi$ state. The accurate r_e structure is useful for comparison with the predictions of *ab initio* calculations.

ACKNOWLEDGMENTS

We thank A. G. Adam and W. Sha (University of New Brunswick) for providing their unpublished experimental results. Support was provided by the Natural Sciences and Engineering Research Council (NSERC) of Canada, the Ministry of Education, Culture, Sports, Science and Technology of Japan (No. 11694055), and the Japan Space Forum (Ground-Based Research for Space Utilization Program).

REFERENCES

1. A. Fowler, *Proc. R. Soc. London A* **79,** 509 (1907).
2. K. R. More and A. H. Parker, *Phys. Rev.* **52,** 1150–1152 (1937).
3. V. R. Rao, *Indian J. Phys.* **23,** 535 (1949).
4. E. A. Shenyavskaya, Y. Y. Kuzyakov, and V. M. Tatevskii, *Opt. Spectrosc.* **12,** 197–199 (1962).
5. A. Chatalic, P. Deschamps, and G. Pannetier, *C. R. Acad. Sci. Paris.* **268,** 1111–1113 (1969).
6. R. L. Diebner and J. G. Kay, *J. Chem. Phys.* **51,** 3547–3554 (1969).
7. K. P. Lanini, Ph.D. thesis, University of Michigan, Ann Arbor, Michigan, 1972.
8. J. G. Phillips and S. P. Davis, *Astrophys. J. Suppl. ser.* **71,** 163–172 (1989).
9. R. S. Ram and P. F. Bernath, *J. Mol. Spectrosc.* **186,** 113–130 (1997).
10. T. Imajo, D. Wang, K. Tanaka, and T. Tanaka, *J. Mol. Spectrosc.* **203,** 216–227 (2000).

11. R. S. Ram, J. R. D. Peers, Y. Teng, A. G. Adam, A. Muntianu, P. F. Bernath, and S. P. Davis, *J. Mol. Spectrosc.* **184,** 186–201 (1997).
12. A. I. Boldyrev and J. Simons, *J. Mol. Spectrosc.* **188,** 138–141 (1998).
13. J. F. Harrison, personal communication.
14. C. Focsa, M. Bencheikh, and L. G. M. Pettersson, *J. Phys. B At. Mol. Opt. Phys.* **31,** 2857–2869 (1998).
15. Y. Sakai, K. Mogi, and E. Miyoshi, *J. Chem. Phys.* **111,** 3989–3994 (1999).
16. R. S. Ram, A. G. Adam, W. Sha, A. Tsouli, J. Liévin, and P. F. Bernath, *J. Chem. Phys.* **114,** 3977–3987 (2001).
17. R. S. Ram and P. F. Bernath, *J. Mol. Spectrosc.* **186,** 355–348 (1997).
18. R. S. Ram and P. F. Bernath, *J. Mol. Spectrosc.* **196,** 235–247 (1999).
19. T. Amano and A. Maeda, *J. Mol. Spectrosc.* **203,** 140–144 (2000).
20. A. G. Adam and W. Sha, to be published.
21. H. Lefebvre-Brion and R. W. Field, "Perturbations in the Spectra of Diatomic Molecules." Academic Press, Orlando, FL, 1986.
22. Y. Shadmi, E. Caspi, and J. Oreg, *J. Res. Natl. Bur. Stand. Sect. A* **73,** 173–189 (1969).
23. J. M. Brown, E. A. Colbourn, J. K. G. Watson, and F. D. Wayne, *J. Mol. Spectrosc.* **74,** 294–318 (1979).
24. J. M. Brown, D. J. Milton, J. K. G. Watson, R. N. Zare, D. L. Albritton, M. Horani, and J. Rostas, *J. Mol. Spectrosc.* **90,** 139–151 (1981).
25. J. M. Brown, A. S. C. Cheung, and A. J. Merer, *J. Mol. Spectrosc.* **124,** 464–475 (1987).
26. E. M. Spain and M. D. Morse, *J. Chem. Phys.* **97,** 4633–4660 (1992).